Published in final edited form as:
J Neuropathol Exp Neurol. 2009 May ; 68(5): 515–524. doi:10.1097/NEN.0b013e3181a24b53.

Alpha-Synuclein S129 Phosphorylation Mutants Do Not Alter Nigrostriatal Toxicity in a Rat Model of Parkinson Disease

Nikolaus R. McFarland, MD, PhD[1], **Zhanyun Fan, MD**[1], **Kui Xu, PhD**[1], **Michael A. Schwarzschild, MD, PhD**[1], **Mel B. Feany, MD, PhD**[2], **Bradley T. Hyman, MD, PhD**[1], and **Pamela J. McLean, PhD**[1]

[1]MassGeneral Institute for Neurodegenerative Disease (MIND), Department of Neurology, Massachusetts General Hospital and Harvard Medical School, Charlestown, Massachusetts.

[2]Department of Pathology, Brigham and Women's Hospital, Harvard Medical School Boston, Massachusetts.

Abstract

Lewy bodies are found in Parkinson disease and related disorders and are extensively phosphorylated at Ser-129, but whether S129 phosphorylation mediates ⟨-synuclein aggregation and neurotoxicity has been controversial. We used recombinant adeno-associated virus (rAAV) to overexpress ⟨-synuclein in the rat nigrostriatal system. Rats were injected with rAAV2/8 expressing either human wild type (wt) or mutant α-synuclein with S129 replaced by alanine (S129A) or aspartate (S129D). Contralateral substantia nigra injections containing empty vector served as controls. Both wt and S129 mutants resulted in significant dopaminergic cell loss in the recipients by 6 weeks but there were only small decreases in nigrostriatal terminal density and tyrosine hydroxylase (TH) expression. There were no significant differences in dopaminergic cell loss, nigrostriatal terminal density, or TH expression among the wt and S129 mutants. Furthermore, we did not observe any differences in ⟨-synuclein aggregate formation or distribution among wt and either S129 mutant. These findings contrast with those from previous studies and suggest that injections of both S129 phosphorylation mutants result in dopaminergic neurotoxicity similar to wt injections. Further study is needed to clarify the effects of these S129 mutants and α-synuclein phosphorylation in mammalian systems.

Keywords

Adeno-associated virus; Dopamine; Lewy bodies; Striatum; Substantia nigra; Tyrosine hydroxylase

INTRODUCTION

Parkinson disease (PD) is the most common neurodegenerative movement disorder and affects about 1% of the population over the age 65. The pathological hallmarks of PD are progressive loss of nigrostriatal dopamine neurons, swollen dystrophic neurites and characteristic filamentous intracellular inclusions called Lewy bodies. These inclusions are not unique to PD as they are also found in related disorders such as dementia with Lewy bodies and multiple system atrophy (1–3). A principal component of Lewy bodies is α-synuclein, a soluble, 140-amino acid protein that is abundantly expressed in the brain and is enriched in synaptic terminals (4). Although its normal function remains unclear, several point mutations in the α-synuclein gene (*PARK1/SNCA*) have been identified and linked to families with autosomal

Correspondence and reprint requests to: Nikolaus R. McFarland, MD, PhD, Building 114, 16th Street – 2400, Charlestown, MA 02129-4404. Tel: 617-726-2299; Fax: 617-724-1480: E-mail: nmcfarland@partners.org.

dominant parkinsonism (5–7). Gene duplication and triplication have also been linked to familial parkinsonism and a gene-dosage effect correlates with earlier disease onset and symptom severity (8–10). The fact that Lewy bodies are also found in these familial forms of parkinsonism further supports a role for α-synuclein in PD pathogenesis (11).

Abnormal folding, aggregation, and deposition of α-synuclein may be key steps in the pathogenesis of sporadic and familial PD (12). α-Synuclein self-aggregates and fibrillizes in vitro forming aggregates suggestive of those seen in Lewy bodies and Lewy neurites (13,14). Moreover, missense mutations in α-synuclein also result in accelerated fibril formation (15, 16) and oligomerization (17). Dose increases (i.e. duplication and triplication) of the α-synuclein gene promote this aggregation and deposition in insoluble fractions, consistent with inclusion formation (18). Animal models of human α-synuclein overexpression likewise demonstrate increased aggregates and neurotoxicity and recapitulate features of PD (19–21).

Epigenetic factors such as phosphorylation also influence α-synuclein fibrillization and aggregate formation. For example, the C-terminal portion of α-synuclein contains several phosphorylation sites (22,23) and there is evidence that Ser-129 phosphorylation accelerates α-synuclein fibrillization and enhances neurotoxicity. S129 is extensively phosphorylated in brains from patients with both sporadic and familial PD (24,25), as well as dementia with Lewy bodies (26). Although a small proportion (less than 5%) of α-synuclein is normally phosphorylated, nearly 90% of α-synuclein in Lewy bodies is phosphorylated at S129. Furthermore, *in vitro* S129 phosphorylation enhances fibril formation (24). In transgenic flies expressing human α-synuclein with mutation of S129 to either alanine (S129A) to prevent phosphorylation or aspartate (S129D) to mimic phosphorylation, blocking S129 phosphorylation suppresses dopamine neuronal loss, whereas S129D enhances α-synuclein neurotoxicity (27). In addition, overexpression of the *Drosophila* G-protein-coupled receptor kinase 2 (GRK2), which selectively phosphorylates α-synuclein at S129, results in enhanced neurotoxicity. Blockade of S129 phosphorylation (S129A) also increases inclusion formation and correlates with decreased α-synuclein neurotoxicity, suggesting that aggregates may be neuroprotective and sequester potentially toxic α-synuclein species. However, a recent study in rats found the opposite and demonstrated that the S129A mutant was more toxic than wild-type human α-synuclein and associated with decreased intracellular aggregates, whereas the phosphomimic S129D appeared to be neuroprotective (28). Thus, whether or not phosphorylation at S129 plays a critical role in mediating α-synuclein-induced dopaminergic neurotoxicity remains uncertain.

In this study we examine the effect of α-synuclein S129 phosphorylation state on dopaminergic neurotoxicity in a rat model of PD. Previous studies have established that viral-vector based overexpression (using either recombinant adeno-associated virus [rAAV] or lentivirus) of human α-synuclein in the rat nigrostriatal system results in progressive dopaminergic cell loss, synuclein-rich aggregates, and dystrophic neurites (29,30). New rAAV serotypes are increasingly being used and they show greater transduction efficiency and delivery of transgene into the nervous system compared to the commonly used rAAV2/2 (31–33). Here, we present new data using rAAV2/8 for delivery of α-synuclein S129 phosphorylation mutants; we find no significant differences in nigrostriatal dopaminergic toxicity or morphology of α-synuclein aggregates among wild type (wt) and S129A/D mutants.

MATERIALS AND METHODS

Virus Production

Construction of rAAV vectors used to express human wild-type α-synuclein was as previously described (34). Overlap extension PCR was used to generate α-synuclein S129 mutants (S129A and S129D) using the mammalian pcDNA-synuclein (human wt, GenBank L08850) vector as

template and previously designed primers (available by request). S129 mutant and wt α-synuclein were then cloned into AAV-CBA-WPRE vector using the subclone internal ribosomal entry site enhanced green fluorescence protein (pIRES2-EGFP) (Clontech, Mountain View, CA). We also constructed an empty vector, AAV-CBA-WPRE, with no transgene (kindly provided by Dr. Miguel Sena-Esteves, Massachusetts General Hospital [MGH], Boston, MA). Recombinant AAV2/8 virus was generated via tripartite transfection of the *cis*-transgene, packaging (*rep* and *cap*) genes, and helper plasmid into HEK 293A cells (Harvard Gene Therapy Initiative, Harvard Medical School). Viral particles were purified by iodixanol density gradient, isolated, and titered by dot blot hybridization. Final titers for virus were for α-synuclein wt 1.4×10^{13} gc/mL, S129D 1.4×10^{13} gc/mL, S129A 7.7×10^{12} gc/mL, and empty vector 1.16×10^{14} gc/mL.

Stereotaxic Viral Injections

All animal protocols and procedures were approved by the MGH Subcommittee on Research Animal Care. The nigrostriatal system is essentially unilateral, thus each animal received bilateral stereotaxic injections of rAAV into the substantia nigra (SN). In most animals, virus with empty vector was injected contralateral to virus encoding human wt or mutant S129A/D α-synuclein. Sprague Dawley rats (300–350 g) were anesthetized, placed in a Kopf stereotax, and bilateral small skull holes were drilled to expose the dura over the injection sites. Coordinates for SN injections from bregma were AP −5.2, ML ± 2.0, and DV −7.4 from the dural surface and targeted the central SN pars compacta (SNc). For each virus, 1.4×10^{10} gc in 2 μL were injected at 0.2 μL/minute using a microinjection pump (Stoelting Co., Wood Dale, IL) with 10 μL Hamilton syringe and 33-gauge needle. After injection the syringe remained in situ for 5 minutes before withdrawal.

Tissue Preparation and Immunohistochemistry

At 2 or 6 weeks post-injection, rats were deeply anesthetized and transcardially perfused with cold 0.1M phosphate buffered saline (PBS, pH 7.4) followed by 4% paraformaldehyde in PBS. Brains from a subset of 6-week-old animals were removed without fixation, and the striatum and midbrain quickly dissected on ice and snap-frozen in isopentane for use in dopamine content measurement and immunoblotting. Perfused brains were postfixed for 24 hours, then cryoprotected in 30% sucrose/PBS, and serially sectioned at 40 μm on a sliding microtome into 12 wells (forebrain and midbrain separately blocked). Sections were collected and stored in cryoprotectant, 30% sucrose and 30% ethylene glycol in PBS, until processed and analyzed. Briefly, free-floating sections were rinsed with PBS, then treated for 3 to 5 minutes with 10% methanol and 3% H_2O_2 to inhibit endogenous peroxidases, permeablized with 0.3% Triton X-100 in PBS, and blocked in 5% normal goat serum. Coronal sections through the striatum and nigra were immunostained with primary antibodies to tyrosine hydroxylase ([TH] 1:10,000 dilution; Millipore, Billerica, MA) or α-synuclein LB509 (1:1000 dilution; Zymed Laboratories, Inc., San Francisco, CA) overnight at 4°C. After washing, immunostaining was visualized with either fluorescent secondary (1:200 dilution; Alexa Fluor 488, Molecular Probes, Eugene, OR; or Cy3, Jackson ImmunoResearch, West Grove, PA) or biotinylated secondary, followed by avidin-biotin (Vectastain Elite Kit, Vector Labs, Burlingame, CA), and 3,3'-diaminobenzidine reaction. Immunostained sections were washed, mounted on Superfrost slides, and coverslipped (GVA mount, Zymed Laboratories, Inc., San Francisco, CA; or Permount, Sigma Chemicals, St. Louis, MO). In some animals, adjacent coronal sections were also Nissl-stained with 0.05% cresyl violet per standard protocols.

Microscopy and Stereology

Immunostained sections were viewed using an Olympus BX51 microscope with bright-field and epifluorescence attachment. Photomicrographs were taken with an Olympus DP70 digital

camera and adjusted only for suitable contrast and brightness. To maintain detail, wide-field images were photo-montaged from high-power photos using Adobe Photoshop CS3. Double-label immunofluorescence images of cells were obtained using a Zeiss LSM510 confocal microscope system. Images were obtained with multi-tracking to minimize spectral overlap.

Nigrostriatal cell loss was assessed by counting TH-immunoreactive cells in the SNc, including the adjacent pars lateralis and caudal dense cell group ventral to the medial lemniscus and retrorubral area, using unbiased stereology according to the optical fractionator principle (35). At least 8 sections (each 240 μm apart) through the SN for each animal were analyzed and counted using the Olympus CAST Stereology System. Sampling intensity was sufficient for a coefficient of error for the counting protocol of less than 0.1.

Striatal TH Terminal Expression

Semiquantitative analysis of TH expression in nigrostriatal terminals at 6 weeks post-injection virus was performed by measurement of optical density of immunofluorescence intensity scans using a Scan Array Express (Perkin Elmer, Boston, MA). All sections for analysis were handled, washed, and immunostained at the same time, using common reagents to minimize inter-animal variability. Striatal sections approximately 1 mm rostral to the decussation of the anterior commissure were immunostained with antibody to TH and fluorescent secondary-Cy3 (Molecular Probes), and scanned using 543-laser excitation. Using ImageJ (NIH), mean gray value of fluorescence intensity within the dorsolateral striatum was obtained for each section and normalized to background, corpus callosum.

Immunoblotting

Striatal and midbrain tissue were separately suspended in 300 μL lysis buffer (50 mM Tris-HCL, pH 7.4; 175 mM NaCl; 5M EDTA, pH 8.0; and protease inhibitor [Roche]) and homogenized on ice for 10 to 15 seconds. Each sample was centrifuged for 15 minutes at 4° C, filtered, and then 1% Triton X-100 added to the lysate. After 1 hour incubation on ice, lysates were centrifuged for 60 minutes at 4°C to collect the triton-X insoluble fraction. Triton-soluble lysate was separated and the insoluble pellet resuspended in 2% SDS-containing lysis buffer (Triton-insoluble fraction), then sonicated for 10 seconds. Protein concentration for each lysate was determined by bicinchoninic acid (BCA) assay. Five μg of each sample were separated on 10% to 20% Trisglycine pre-cast gel (Invitrogen, San Diego, CA), transferred to polyvinylidene diflouride (PVDF), and immunoblotted for TH (mouse TH-2 antibody, Sigma) or α-synuclein (mouse Syn1, BD Transduction Laboratories, or Syn (LB509), Zymed, antibody). All blots were immunostained for glyceraldehyde-3-phosphate dehydrogenase (GAPDH) (rabbit antibody, Abcam, Cambridge, MA) as loading control. In some cases samples for each condition were pooled. Immunoblotted α-synuclein, TH and GAPDH were detected with secondary antibody conjugated to horseradish peroxidase (HRP) and reacted with ECL (GE Healthcare, Waukesha, WI), per protocol. Films were scanned using a FluorChem system and analyzed with ImageJ software (NIH). TH and α-synuclein content for each sample was normalized to GAPDH.

Dopamine Content

Striatal tissue was thawed, homogenized, and mixed in lysis buffer with dihydrobenzylamine added as internal control. Dopamine and 3,4-dihydroxyphenlyacetic acid (DOPAC) were measured by high performance liquid chromatography (HPLC) with electrochemical detection and normalized to protein content per sample (36).

Statistics

All data were expressed as group mean ± SEM. Stereological estimates of nigral TH cell survival, mean striatal terminal density, and dopamine measurements were analyzed using one-way ANOVA with Bonferonni's multiple comparison post-hoc (Prism GraphPad 4.03, San Diego, CA) unless otherwise stated.

RESULTS

We used the pseudotyped rAAV 2/8 for delivery of transgene because recent rAAV serotype comparisons have shown increased transduction efficiency over that of rAAV2/2 (33,36). Transgene expression for rAAV2/8 is also markedly enhanced over rAAV2/2 and rapidly reaches a steady state by 2 to 4 weeks (37,38). Rat SN were stereotaxically injected with equal volume and genome copies of rAAV vector encoding either human wt or S129 phosphorylation mutant (S129A for substitution to alanine, or S129D for aspartate) α-synuclein, followed by an internal ribosomal entry site (IRES) and the reporter gene EGFP, resulting in bicistronic expression. To control for possible viral toxicity and injection effects, the contralateral SN of several rats was injected with empty rAAV vector and used as an internal control. Based on preliminary experiments with rAAV2/8, its rapid transgene expression and spread, we selected 2-and 6-week time points post-injection for analysis of wt and S129A/D α-synuclein toxicity in the nigrostriatal system.

The patterns of transgene expression for all rAAV were similar. For α-synuclein viruses, EGFP expression marked cells transduced with rAAV in the SN. All cells with EGFP co-expressed α-synuclein as assessed by double immunofluorescence. rAAV2/8 was neurotrophic; we did not observe transduction of glial elements. At 2 and 6 weeks post-injection, EGFP expression was widespread for α-synuclein rAAV and included cells not only in the SNc, but also in the adjacent pars reticulata (SNr), ventral tegmental nucleus, and a portion of the ventral mesencephalic reticular formation (Fig. 1). These findings are consistent with the reported enhanced transduction efficiency of rAAV2/8 compared to rAAV2/2 in the SN (33,34,37).

In addition to cellular expression of α-synuclein within the SN, immunostaining for human α-synuclein using the LB509 antibody (specific for amino acid residues 115–122) also demonstrated extensive transport of α-synuclein to nigrostriatal terminals (Fig. 2). Animals without extensive nigrostriatal labeling suggested failed or misplaced injections and were excluded from the analysis. Synuclein-positive terminals were widespread and found throughout the dorsal striatum (caudatoputamen), extending rostrally to the striatal pole and several millimeters caudal to the anterior commissure. These findings are consistent with the topographic distribution of nigrostriatal projections (39) and confirm transduction of a large proportion of SNc neurons for each case. Double labeling of SN with antibodies to α-synuclein (or GFP) and TH also demonstrated that rAAV injections transduced a majority of dopaminergic nigrostriatal neurons in the SNc and adjacent regions (data not shown).

Viral Expression

To assess rAAV α-synuclein expression levels for wt, S129A and S129D mutants, we performed Western blot analyses on striatal and midbrain extracts from 3 animals per group obtained at 6 weeks post-injection and compared these to extracts from the contralateral hemisphere injected with empty vector control. Blots from samples taken from wt, S129A, and S129D α-synuclein recipients probed with the LB509 synuclein antibody demonstrated strong human α-synuclein expression ipsilateral to the injection, as expected. We also probed blots with the Syn-1 antibody (BD Transduction, San Jose, CA), which recognizes both endogenous rat and human α-synuclein, to estimate the level of human α-synuclein overexpression for each rAAV compared to endogenous levels (Fig. 3). Comparison of the α-synuclein injected side

to the contralateral striatum or midbrain, empty rAAV vector control, revealed levels of α-synuclein overexpression with a mean ratio (ipsilateral/contralateral side) of approximately twice that of endogenous rat α-synuclein.

Comparison of Nigrostriatal Toxicity

Unbiased stereological estimates of TH-positive cells in the SN were performed at 2 and 6 weeks post-injection of rAAV expressing wt or mutant, S129A or S129D, α-synuclein and compared to empty vector injections. In preliminary studies, subtle TH cell loss was observed at 2 weeks in both wt and mutant S129A and S129D groups (n = 2 to 3 for each group). These findings were somewhat surprising given the early time point, but dopaminergic neurotoxicity for S129A has been observed as early as 4 weeks (28). Qualitative comparison of TH cell loss with cresyl violet-stained sections confirmed proportional nigral cell loss and gliosis. Given the modest extent of cell loss at 2 weeks, we examined a larger cohort (6 to 10 per group) at 6 weeks to further compare toxicity of wt and S129 mutant α-synucleins.

At 6 weeks post-injection there was TH cell loss evident in the SNc for both wt and S129 mutant α-synuclein groups (Fig. 4). Cell loss, as opposed to TH-phenotype loss, was confirmed by analysis of Nissl-stained sections and qualitative comparison with nigral TH cell loss. Stereological estimates of remaining TH cells in the SN demonstrated significant cell loss compared to empty vector control for wt (20.5 ± 6.8%, $p < 0.05$), S129A (29.9 ± 2.4%, $p < 0.001$), and S129D (27.0 ± 6.7%, $p < 0.01$) mutants ($F[3,24] = 9.96$, $p = 0.0002$) (Fig. 5A). The mean TH cell loss was 25.8% and ranged from 7% to 45% for all animals analyzed. Post-hoc analysis revealed no significant differences in TH cell counts between wt, S129A, or S129D. Qualitative comparison of nigral TH staining at 6 weeks also did not differ.

Nigrostriatal TH and Dopamine Content

Immunostaining of striatal sections for TH did not show nigrostriatal terminal loss at 2 weeks. By contrast, at 6 weeks TH-immunostaining revealed loss of terminal density in the dorsal striatum for both S129A and S129D compared to wt recipients (Fig. 2). Semiquantitative analysis, using scan array measurement of immunofluorescence optical density also revealed small decreases relative to control in dorsal striatal TH-positive terminal density for wt and mutant S129A and S129D recipients, but these findings did not achieve statistical significance (Fig. 5B). Relative side-to-side comparisons of recipients with internal empty vector control showed a similar trend of decreased dorsal striatal TH-positive terminal density for S129A and S129D mutant animals but also did not achieve significance.

To investigate potential changes in striatal dopaminergic innervation further, we also quantified striatal dopamine content at 6 weeks post-injection via HPLC fractionation and electrochemical detection. Dopamine was extracted from striatal tissue ipsilateral to the SN injection of either wt or mutant (S129A or S129D) α-synuclein and compared to that extracted from the contralateral control striatum (SN injected with empty rAAV vector). In wt recipients, the striatal dopamine content and levels of its metabolite, DOPAC, did not differ (Fig. 5C). In contrast, relative dopamine content for S129A did significantly decrease, mean ratio (ipsilateral/contralateral striatum) 0.66 ± 0.04 ($p = 0.006$, one sample *t*-test for hypothesized ratio of 1). Dopamine levels also decreased for S129D (mean ratio 0.59 ± 0.15), but did not achieve statistical significance ($p = 0.055$). Similarly, striatal DOPAC content for both S129A and S129D recipients demonstrated a trend toward decrease but were not significant. These results are consistent with the loss of 25% of TH-positive neurons in the SN.

Synuclein Toxicity, Cellular Aggregates, and Terminal Morphology

Examination of sections stained for human α-synuclein (LB509) at 2 and 6 weeks using bright-field and confocal microscopy revealed progressive changes in nigral cell morphology.

Synuclein-positive cells in wt and mutant S129A and S129D cases were densely immunostained throughout the nucleus and cytoplasm (Fig. 6). A subset of cells contained synuclein-positive aggregates at 6 weeks. Some larger cell aggregates co-stained for α-synuclein and ubiquitin. There were no qualitative differences in aggregate size or distribution between wt and S129A or S129A cases. Transduced cells frequently had dystrophic process as previously described (29). Examination of nigrostriatal terminals immunostained for human α-synuclein also showed dystrophic changes and neurites, but no qualitative differences were noted between wt, S129A or S129D animals.

DISCUSSION

We examined the role of α-synuclein phosphorylation at Ser-129 by comparing the effects of overexpression of human wt and mutant α-synuclein S129A (alanine blocks phosphorylation) and S129D (mimics constitutive phosphorylation) in the rat nigrostriatal system. A targeted viral vector-based approach with rAAV2/8 was used to overexpress α-synuclein in the SNc. Neither Ser-129 α-synuclein mutant appeared to significantly alter dopaminergic nigrostriatal toxicity in the rat PD model. At 2 weeks, early neurodegenerative changes and TH cell loss were apparent, and by 6 weeks overexpression of wt and S129A and S129D mutants resulted in significant (20%–30%) nigral dopaminergic cell loss (confirmed on Nissl-stained sections) compared to empty vector control. There were, however, no significant differences in dopaminergic nigrostriatal cell toxicity between wt, S129A, or S129D α-synuclein at 6 weeks. Furthermore, the size and distribution of α-synuclein aggregates did not differ among wt and either S129 mutant. Consistent with these findings, we did not detect major changes in striatal TH-terminal density or expression, although striatal dopamine content was decreased for S129A and S129D. The normal striatal dopamine levels for wt α-synuclein are not surprising because over 6 weeks non-geriatric rodents have the ability to recover dopamine content after nigrostriatal lesion such as that caused by 1-methyl-4-phenyl-1,2,3,6-tetrahydropyridine (MPTP) (40). The lack of recovery of dopamine content for both S129 mutants thus may suggest a decrease in functional neurochemical compensation or plasticity. Morphologically, α-synuclein-positive nigrostriatal terminals in S129 recipients did not differ significantly from those of wt but S129 mutants may alter dopamine release and synaptic function since these are putatively regulated by α-synuclein (41).

These findings contrast with those from previous studies in similar *Drosophila* and rat PD models that also compared wt α-synuclein and S129A and S129D phosphorylation mutants (27,28). In the fly, S129D was more toxic to dopamine cells and S129A was not only protective, but also associated with an increase in α-synuclein aggregates. Recent data in rats found the opposite result and demonstrated increased toxicity for S129A and possible neuroprotective effects for S129D (28). Toxicity was, however, similarly associated with a decrease in large, insoluble α-synuclein aggregates whereas neuroprotection correlated with the presence of cytoplasmic inclusions. By contrast, we observed no differences in toxicity or aggregate formation for wt α-synuclein or the phosphorylation mutants S129A and S129D in the rat.

Differences in study design may in part explain these differing results among studies. We used rAAV2/8 to deliver and overexpress α-synuclein in the rat SN, whereas Gorbatyuk et al used a different serotype, rAAV2/5 (28). Both of these rAAVs show enhanced transduction efficiency (i.e. increase in cell number and volume transduced) over that of rAAV2/2 in the rodent nigrostriatal system (33,38,42). However, rAAV2/8 results in higher transgene expression than other rAAV serotypes, including 2/2 and 2/5 (37). One concern is that elevated levels of α-synuclein expression from high-titer AAV2/8 injections may mask differences in toxicity between wt and the S129 mutants. Therefore, we injected a moderate dose of each virus (1.4×10^{10} gc), resulting in only 20% to 30% nigral TH cell loss at 6 weeks. Using a similar dose of AAV2/5, Gorbatyuk et al reported 40% to 60% cell loss for both wt and S129A,

albeit at 8 weeks post-injection. Moreover, Western blot estimates of human α-synuclein expression compared to endogenous rat α-synuclein were also lower (only 2-fold) than that previously reported. These findings suggest that the amount of virus injected and, indirectly, the levels of α-synuclein expression in our study did not "saturate" the system. The fact that we saw toxicity in S129D recipients also argues that the viral dose was not too low, since previously it appeared to be less toxic than the wt (28).

Another difference between this and previous studies is the length of viral incubation. The time course for expression of the transgene is similar for both rAAV 2/5 and 2/8, although perhaps a bit more rapid for rAAV2/8 (38). The 2 and 6 week time points for analysis we chose may have been too early to detect differences in toxicity among wt and S129 mutants. Even at 4 weeks, however, toxicity was noted for S129A by Gorbatyuk et al and was evident by 2 weeks in this study (28). Moreover, by 6 weeks, the wt and both S129 mutant recipients showed significant dopaminergic cell toxicity.

Recent *in vitro* data on S129 phosphorylation and phosphomimics (e.g. S129D/E) may also help to explain differences in results from rat and fly PD models. S129 phosphorylation increases α-synuclein conformational flexibility and appears to inhibit fibril formation. Although they are designed as phosphomimics, S129D/E do not exactly reproduce the effects of native phosphorylation (43). S129 phosphomimics only demonstrate local changes in conformational dynamics and form fibrils similar to those formed by wt in vitro but not as rapidly as S129A. Consistent with these findings we found similar toxicity for wt and S129D α-synuclein. Rapid fibrillization due to S129A presumably leads to increased α-synuclein aggregate formation that is thought to sequester toxic species. This hypothesis is supported by reduced S129A toxicity and increased α-synuclein inclusions seen in the fly (27). Contradictory results for S129A are, however, seen in the rat (28), possibly suggesting that while fibrils form, the S129A mutant in a mammalian system may also enhance formation of toxic α-synuclein oligomers. Together, these findings emphasize the importance of phosphorylation at S129 as a regulator of α-synuclein function but do not fully clarify its effects on toxicity.

Increasing evidence suggests that large α-synuclein aggregates may be neuroprotective and that S129 phosphorylation plays a role in aggregate formation (44). A high proportion of α-synuclein in Lewy bodies is phosphorylated at S129 (24,25). Furthermore, co-expression of human α-synuclein and protein kinases, such as G-protein-receptor kinase 5 (GRK5)—one of many kinases that phosphorylate at S129 (27,45)—is associated with α-synuclein aggregate formation in cell culture (46). Recent data indicate, however, that S129 phosphorylation can also inhibit fibril formation and α-synuclein oligomerization but with longer incubation times fibrillary aggregates such as those found in Lewy bodies eventually form (43). Lingering questions remain as to what influences α-synuclein phosphorylation, when it occurs (before, during or after fibrillization and aggregate formation), and how it may mediate neurotoxicity.

Several kinases phosphorylate α-synuclein at S129, including casein kinases 1 and 2, and GRK2 and 5 (22,45,47), but specific phosphatases have yet to be identified. Regulation of the α-synuclein phosphorylation state in vivo thus remains unclear, in particular due to the multiple cellular compartments in which α-synuclein is found. Phosphorylation of α-synuclein by GRKs is enhanced by phospholipids (45). Liposomal binding of α-synuclein and GRK appears to increase its kinase activity (48). α-Synuclein phosphorylation by casein kinase 2 is similarly enhanced by liposomes. There is also evidence for Ca^{2+}/calmodulin interaction with GPK5 and activation of α-synuclein phosphorylation (49). Further study is necessary to identify other specific kinases and protein and membrane interactions involved in α-synuclein phosphorylation.

The function of α-synuclein remains largely unknown and further complicates our understanding of its role in PD pathophysiology. Putative functions include regulation of synaptic dopamine transport (41), vesicle formation and trafficking (51), mitochondrial function (41,50), and nuclear transcription (51). How α-synuclein phosphorylation affects these functions is unclear, but disruption in any one of these could lead to dysfunction and potential neurotoxicity. Findings presented here suggest that the phosphorylation state at S129 and its effects *in vivo* are more complex than previously thought and that it may not play a critical role in mediating dopaminergic toxicity. A better understanding of α-synuclein phosphorylation and aggregate formation is clearly needed and will help target novel therapies.

Acknowledgments

This work was supported by NIH NS038372A-08 (B.T.H.) and DOD W81XWH-04-1-0881 (M.A.S.). N.R.M. is supported by an American Parkinson Disease Association (APDA) and the Koch Jr. Fellowship.

REFERENCES

1. Baba M, Nakajo S, Tu PH, et al. Aggregation of alpha-synuclein in Lewy bodies of sporadic Parkinson's disease and dementia with Lewy bodies. Am J Pathol 1998;152:879–884. [PubMed: 9546347]
2. Spillantini MG, Schmidt ML, Lee VM, et al. Alpha-synuclein in Lewy bodies. Nature 1997;388:839–840. [PubMed: 9278044]
3. Tu PH, Galvin JE, Baba M, et al. Glial cytoplasmic inclusions in white matter oligodendrocytes of multiple system atrophy brains contain insoluble alpha-synuclein. Ann Neurol 1998;44:415–422. [PubMed: 9749615]
4. Iwai A, Masliah E, Yoshimoto M, et al. The precursor protein of non-A beta component of Alzheimer's disease amyloid is a presynaptic protein of the central nervous system. Neuron 1995;14:467–475. [PubMed: 7857654]
5. Kruger R, Kuhn W, Muller T, et al. Ala30Pro mutation in the gene encoding alpha-synuclein in Parkinson's disease. Nat Genet 1998;18:106–108. [PubMed: 9462735]
6. Polymeropoulos MH, Lavedan C, Leroy E, et al. Mutation in the alpha-synuclein gene identified in families with Parkinson's disease. Science 1997;276:2045–2047. [PubMed: 9197268]
7. Zarranz JJ, Alegre J, Gomez-Esteban JC, et al. The new mutation, E46K, of alpha-synuclein causes Parkinson and Lewy body dementia. Ann Neurol 2004;55:153–156. [PubMed: 14755715]
8. Chartier-Harlin MC, Kachergus J, Roumier C, et al. Alpha-synuclein locus duplication as a cause of familial Parkinson's disease. Lancet 2004;364:1167–1169. [PubMed: 15451224]
9. Singleton AB, Farrer M, Johnson J, et al. alpha-Synuclein locus triplication causes Parkinson's disease. Science 2003;302:841. [PubMed: 14593171]
10. Wood-Kaczmar A, Gandhi S, Wood NW. Understanding the molecular causes of Parkinson's disease. Trends Mol Med 2006;12:521–528. [PubMed: 17027339]
11. Kotzbauer PT, Giasson BI, Kravitz AV, et al. Fibrillization of alpha-synuclein and tau in familial Parkinson's disease caused by the A53T alpha-synuclein mutation. Exp Neurol 2004;187:279–288. [PubMed: 15144854]
12. Feany MB. New genetic insights into Parkinson's disease. N Engl J Med 2004;351:1937–1940. [PubMed: 15525720]
13. Conway KA, Harper JD, Lansbury PT Jr. Fibrils formed in vitro from alpha-synuclein and two mutant forms linked to Parkinson's disease are typical amyloid. Biochemistry 2000;39:2552–2563. [PubMed: 10704204]
14. Hashimoto M, Hsu LJ, Sisk A, et al. Human recombinant NACP/alpha-synuclein is aggregated and fibrillated in vitro: Relevance for Lewy body disease. Brain Res 1998;799:301–306. [PubMed: 9675319]
15. Conway KA, Harper JD, Lansbury PT. Accelerated in vitro fibril formation by a mutant alpha-synuclein linked to early-onset Parkinson disease. Nat Med 1998;4:1318. [PubMed: 9809558]
16. Greenbaum EA, Graves CL, Mishizen-Eberz AJ, et al. The E46K mutation in alpha-synuclein increases amyloid fibril formation. J Biol Chem 2005;280:7800. [PubMed: 15632170]

17. Conway KA, Lee SJ, Rochet JC, et al. Accelerated oligomerization by Parkinson's disease linked alpha-synuclein mutants. Ann NY Acad Sci 2000;920:42–45. [PubMed: 11193175]
18. Miller DW, Hague SM, Clarimon J, et al. Alpha-synuclein in blood and brain from familial Parkinson disease with SNCA locus triplication. Neurology 2004;62:1835–1838. [PubMed: 15159488]
19. Feany MB, Bender WW. A Drosophila model of Parkinson's disease. Nature 2000;404:394–398. [PubMed: 10746727]
20. Chesselet MF. In vivo alpha-synuclein overexpression in rodents: A useful model of Parkinson's disease? Exp Neurol 2008;209:22–27. [PubMed: 17949715]
21. Springer W, Kahle PJ. Mechanisms and models of alpha-synuclein-related neurodegeneration. Curr Neurol Neurosci Rep 2006;6:432–436. [PubMed: 16928354]
22. Okochi M, Walter J, Koyama A, et al. Constitutive phosphorylation of the Parkinson's disease associated alpha-synuclein. J Biol Chem 2000;275:390–397. [PubMed: 10617630]
23. Ellis CE, Schwartzberg PL, Grider TL, et al. alpha-synuclein is phosphorylated by members of the Src family of protein-tyrosine kinases. J Biol Chem 2001;276:3879–3884. [PubMed: 11078745]
24. Fujiwara H, Hasegawa M, Dohmae N, et al. alpha-Synuclein is phosphorylated in synucleinopathy lesions. Nat Cell Biol 2002;4:160–164. [PubMed: 11813001]
25. Anderson JP, Walker DE, Goldstein JM, et al. Phosphorylation of Ser-129 is the dominant pathological modification of alpha-synuclein in familial and sporadic Lewy body disease. J Biol Chem 2006;281:29739–29752. [PubMed: 16847063]
26. Saito Y, Kawashima A, Ruberu NN, et al. Accumulation of phosphorylated alpha-synuclein in aging human brain. J Neuropathol Exp Neurol 2003;62:644–654. [PubMed: 12834109]
27. Chen L, Feany MB. Alpha-synuclein phosphorylation controls neurotoxicity and inclusion formation in a Drosophila model of Parkinson disease. Nat Neurosci 2005;8:657–663. [PubMed: 15834418]
28. Gorbatyuk OS, Li S, Sullivan LF, et al. The phosphorylation state of Ser-129 in human alpha-synuclein determines neurodegeneration in a rat model of Parkinson disease. Proc Natl Acad Sci U S A 2008;105:763–768. [PubMed: 18178617]
29. Kirik D, Rosenblad C, Burger C, et al. Parkinson-like neurodegeneration induced by targeted overexpression of alpha-synuclein in the nigrostriatal system. J Neurosci 2002;22:2780–2791. [PubMed: 11923443]
30. Lo Bianco C, Ridet JL, Schneider BL, et al. alpha -Synucleinopathy and selective dopaminergic neuron loss in a rat lentiviral-based model of Parkinson's disease. Proc Natl Acad Sci USA 2002;99:10813–10818. [PubMed: 12122208]
31. Gao G, Vandenberghe LH, Wilson JM. New recombinant serotypes of AAV vectors. Curr Gene Ther 2005;5:285–297. [PubMed: 15975006]
32. Howard DB, Powers K, Wang Y, et al. Tropism and toxicity of adeno-associated viral vector serotypes 1, 2, 5, 6, 7, 8, and 9 in rat neurons and glia in vitro. Virology. 2007[Epub ahead of print]
33. Taymans JM, Vandenberghe LH, Haute CV, et al. Comparative analysis of adeno-associated viral vector serotypes 1, 2, 5, 7, and 8 in mouse brain. Hum Gene Ther 2007;18:195–206. [PubMed: 17343566]
34. St Martin JL, Klucken J, Outeiro TF, et al. Dopaminergic neuron loss and up-regulation of chaperone protein mRNA induced by targeted over-expression of alpha-synuclein in mouse substantia nigra. J Neurochem 2007;100:1449–1457. [PubMed: 17241127]
35. West MJ, Slomianka L, Gundersen HJ. Unbiased stereological estimation of the total number of neurons in the subdivisions of the rat hippocampus using the optical fractionator. Anat Rec 1991;231:482–497. [PubMed: 1793176]
36. Broekman ML, Comer LA, Hyman BT, et al. Adeno-associated virus vectors serotyped with AAV8 capsid are more efficient than AAV-1 or -2 serotypes for widespread gene delivery to the neonatal mouse brain. Neuroscience 2006;138:501–510. [PubMed: 16414198]
37. Klein RL, Dayton RD, Leidenheimer NJ, et al. Efficient neuronal gene transfer with AAV8 leads to neurotoxic levels of tau or green fluorescent proteins. Mol Ther 2006;13:517–527. [PubMed: 16325474]
38. Reimsnider S, Manfredsson FP, Muzyczka N, et al. Time course of transgene expression after intrastriatal pseudotyped rAAV2/1, rAAV2/2, rAAV2/5, and rAAV2/8 transduction in the rat. Mol Ther 2007;15:1504–1511. [PubMed: 17565350]

39. Maurin Y, Banrezes B, Menetrey A, et al. Three-dimensional distribution of nigrostriatal neurons in the rat: Relation to the topography of striatonigral projections. Neuroscience 1999;91:891–909. [PubMed: 10391469]
40. Schmidt N, Ferger B. Neurochemical findings in the MPTP model of Parkinson's disease. J Neural Transm 2001;108:1263–1282. [PubMed: 11768626]
41. Wersinger C, Prou D, Vernier P, et al. Modulation of dopamine transporter function by alpha-synuclein is altered by impairment of cell adhesion and by induction of oxidative stress. FASEB J 2003;17:2151–2153. [PubMed: 12958153]
42. Burger C, Gorbatyuk OS, Velardo MJ, et al. Recombinant AAV viral vectors pseudotyped with viral capsids from serotypes 1, 2, and 5 display differential efficiency and cell tropism after delivery to different regions of the central nervous system. Mol Ther 2004;10:302–317. [PubMed: 15294177]
43. Paleologou KE, Schmid AW, Rospigliosi CC, et al. Phosphorylation at Ser-129 but not the phosphomimics S129E/D inhibits the fibrillation of alpha-synuclein. J Biol Chem 2008;283:16895–16905. [PubMed: 18343814]
44. Cookson MR. The biochemistry of Parkinson's disease. Annu Rev Biochem 2005;74:29–52. [PubMed: 15952880]
45. Pronin AN, Morris AJ, Surguchov A, et al. Synucleins are a novel class of substrates for G protein-coupled receptor kinases. J Biol Chem 2000;275:26515–26522. [PubMed: 10852916]
46. Arawaka S, Wada M, Goto S, et al. The role of G-protein-coupled receptor kinase 5 in pathogenesis of sporadic Parkinson's disease. J Neurosci 2006;26:9227–9238. [PubMed: 16957079]
47. Wakamatsu M, Ishii A, Ukai Y, et al. Accumulation of phosphorylated alpha-synuclein in dopaminergic neurons of transgenic mice that express human alpha-synuclein. J Neurosci Res 2007;85:1819–1825. [PubMed: 17465029]
48. Pronin AN, Carman CV, Benovic JL. Structure-function analysis of G protein-coupled receptor kinase-5. Role of the carboxyl terminus in kinase regulation. J Biol Chem 1998;273:31510–31518. [PubMed: 9813065]
49. Chuang TT, Paolucci L, De Blasi A. Inhibition of G protein-coupled receptor kinase subtypes by Ca2+/calmodulin. J Biol Chem 1996;271:28691–28696. [PubMed: 8910504]
50. Parihar MS, Parihar A, Fujita M, et al. Mitochondrial association of alpha-synuclein causes oxidative stress. Cell Mol Life Sci 2008;65:1272–1284. [PubMed: 18322646]
51. Kontopoulos E, Parvin JD, Feany MB. Alpha-synuclein acts in the nucleus to inhibit histone acetylation and promote neurotoxicity. Hum Mol Genet 2006;15:3012–3023. [PubMed: 16959795]

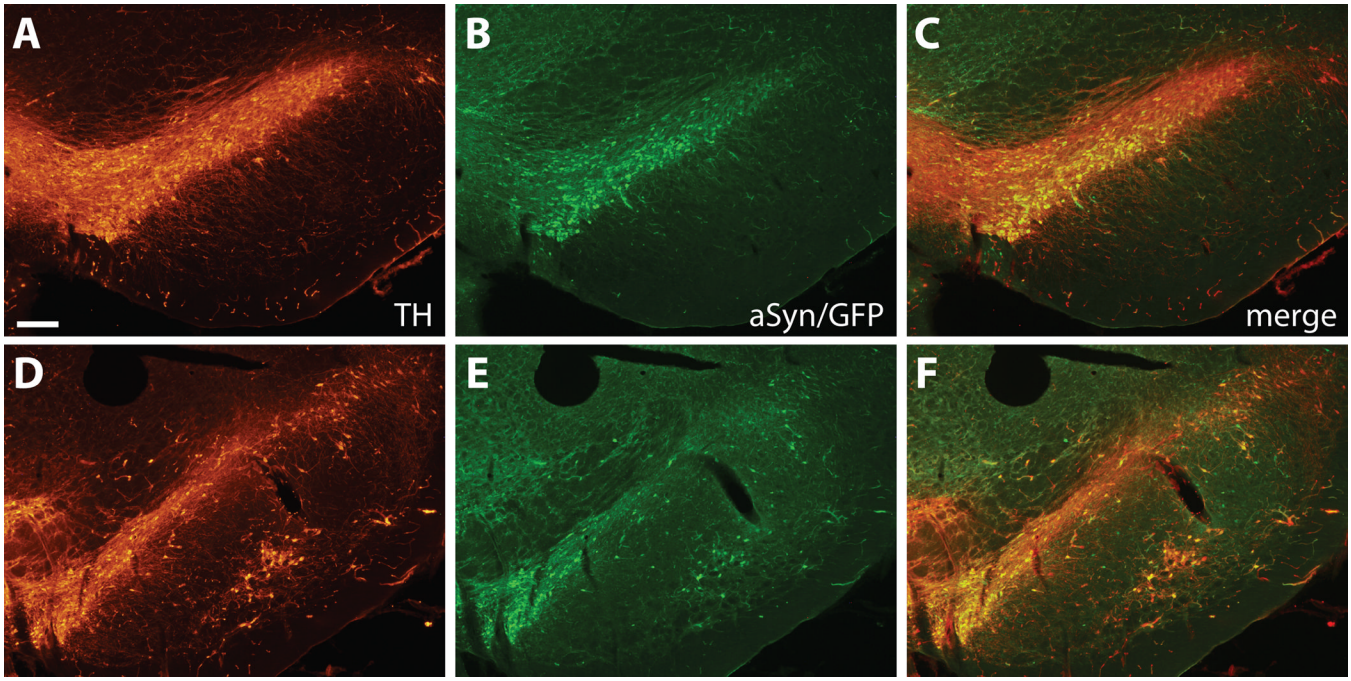

Figure 1.
Immunofluorescence staining of substantia nigra (SN) injected with rAAV2/8 expressing wt α-synuclein and internal ribosomal entry site-enhanced green fluorescent protein (EGFP). Tyrosine hydroxylase (TH) staining shows the distribution of dopaminergic SN neurons at representative rostral (**A–C**) and caudal (**D–F**) levels. GFP-positive transduced cells are widely distributed throughout the SN and almost exclusively colocalize with TH-positive neurons. Bar: 250 μm.

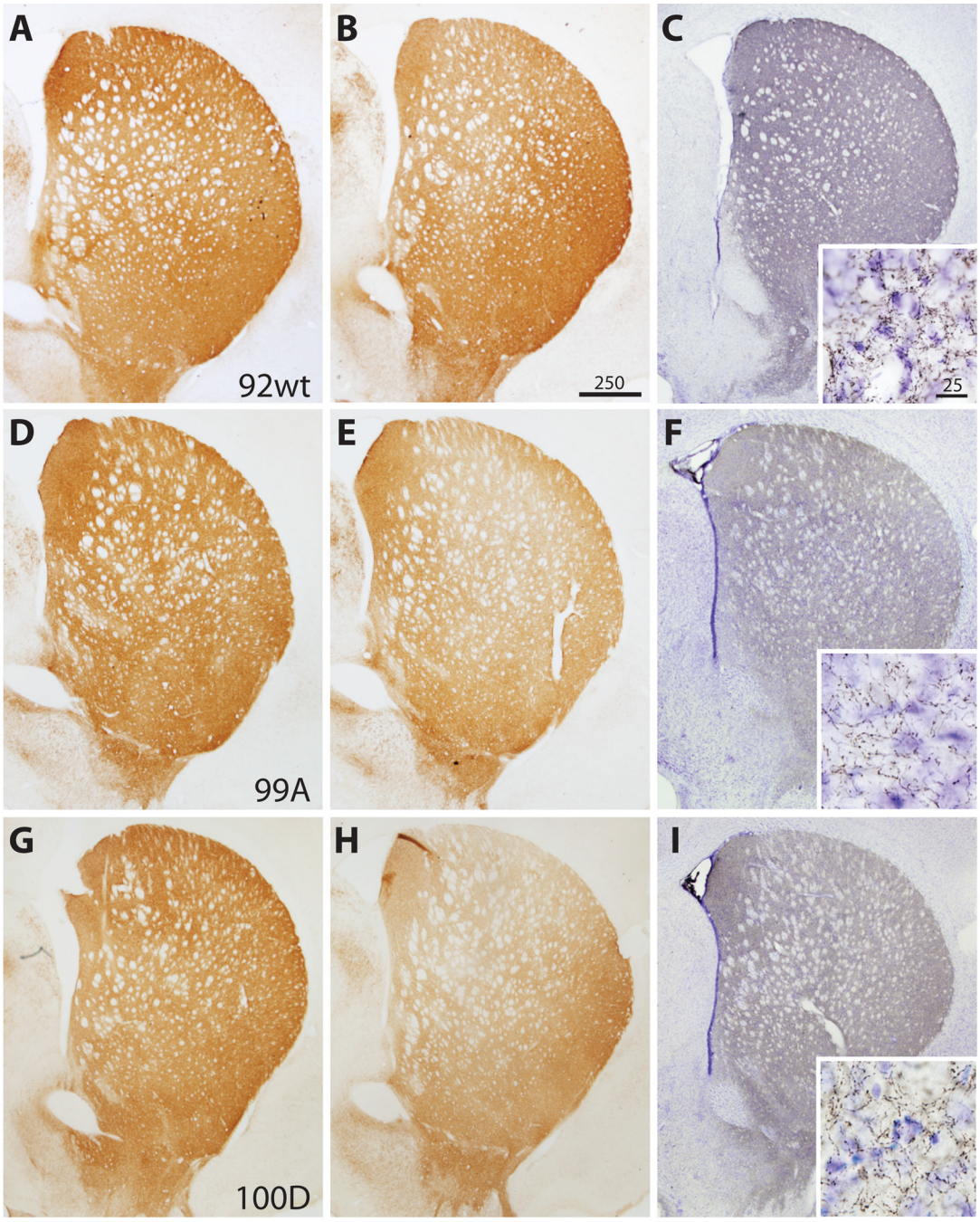

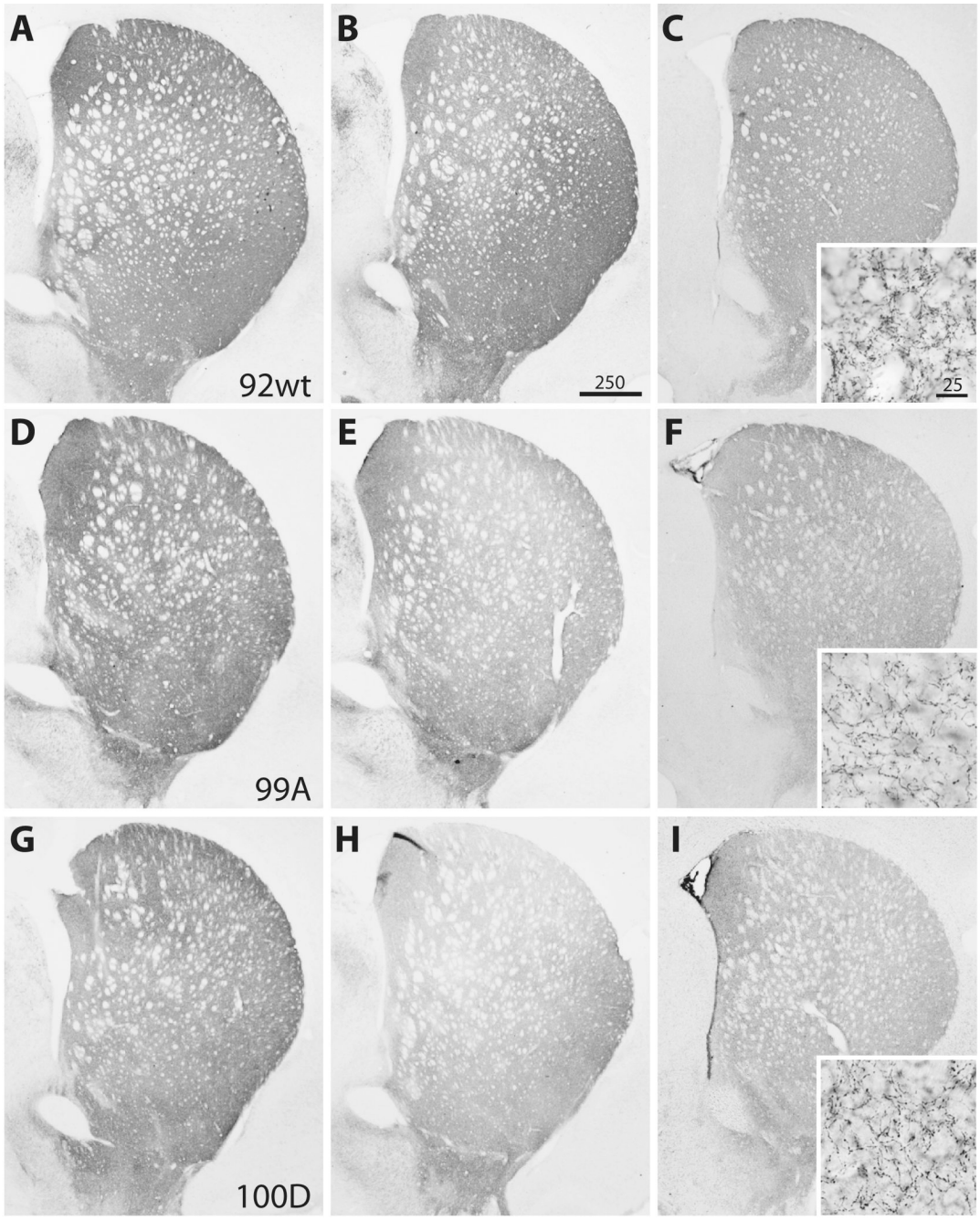

Figure 2.

The distribution of nigrostriatal terminals immunostained for tyrosine hydroxylase (TH) and human α-synuclein (LB509) at 6 weeks post-injection. Columns 1 and 2 compare striatal TH terminal labeling after empty vector control (**A, D, G**) and ⟨-synuclein (**B, E, H**) injection in the same animal. There is striatal TH terminal loss in the dorsal striatum on the side of ⟨-synuclein injection that appears more prominent for both S129 mutants (**E, H**) than for the wt (**B**). The distribution of α-synuclein-positive (LB509 antibody) striatal terminals (**C, F, I**) is similar among wild type (wt) and mutant recipient animals. Insets reveal high-power detail of ⟨-synuclein-positive nigrostriatal terminals. Bars indicate respective magnification (∫m).

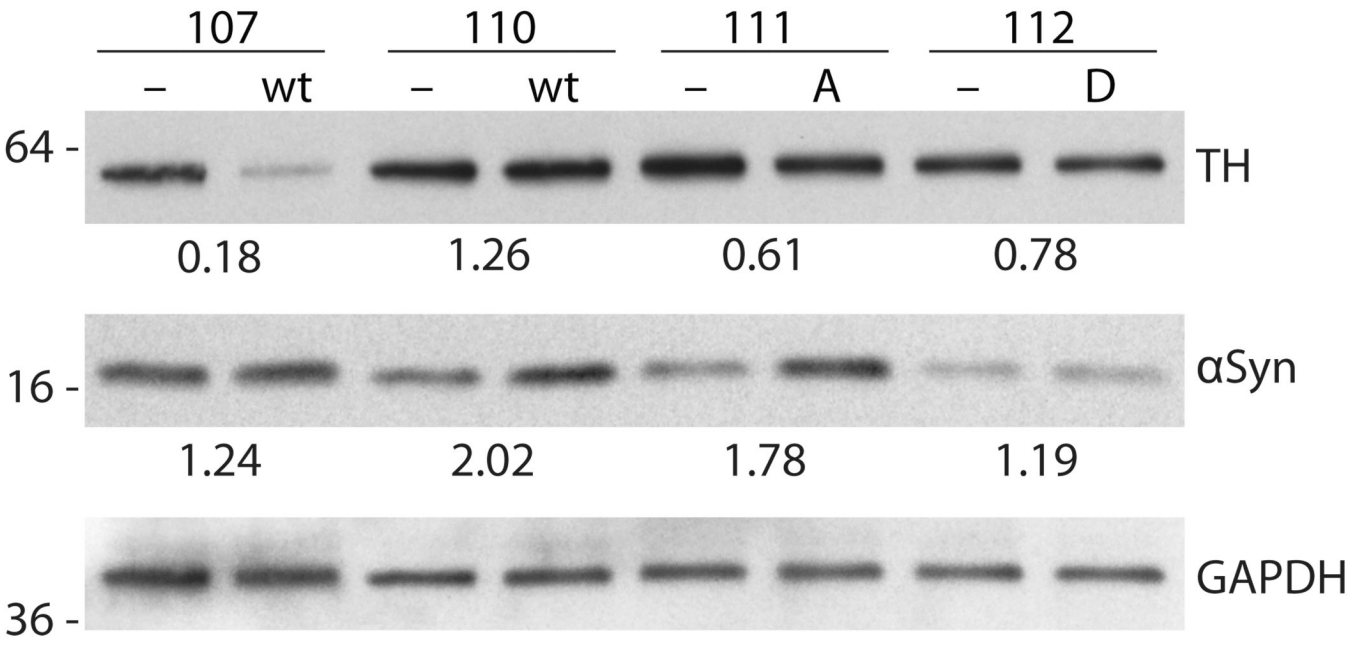

Figure 3.

Measurement of ⟨-synuclein and tyrosine hydroxylase (TH) expression in midbrain tissue 6 weeks post-viral injection. Western blots show samples from midbrain ipsilateral to ⟨-synuclein (wild type [wt], S129A [A], and S129D [D]) injection and are compared to protein extracts from the contralateral midbrain injected with empty vector (−) control in the same animal. Protein from left and right midbrain samples was probed with primary antibody to ⟨-synuclein and TH, followed by secondary HRP-conjugated antibody and ECL detection. Bands were quantified and normalized to GAPDH loading control. The ratio of ⟨-synuclein and TH for the α-synuclein (ipsilateral) versus empty vector (contralateral) side was calculated for each animal. Blots show ⟨-synuclein overexpression for most animals, but there was variable expression as shown for the 2 wt samples. Decreased TH expression is also shown for wt and S129 mutants.

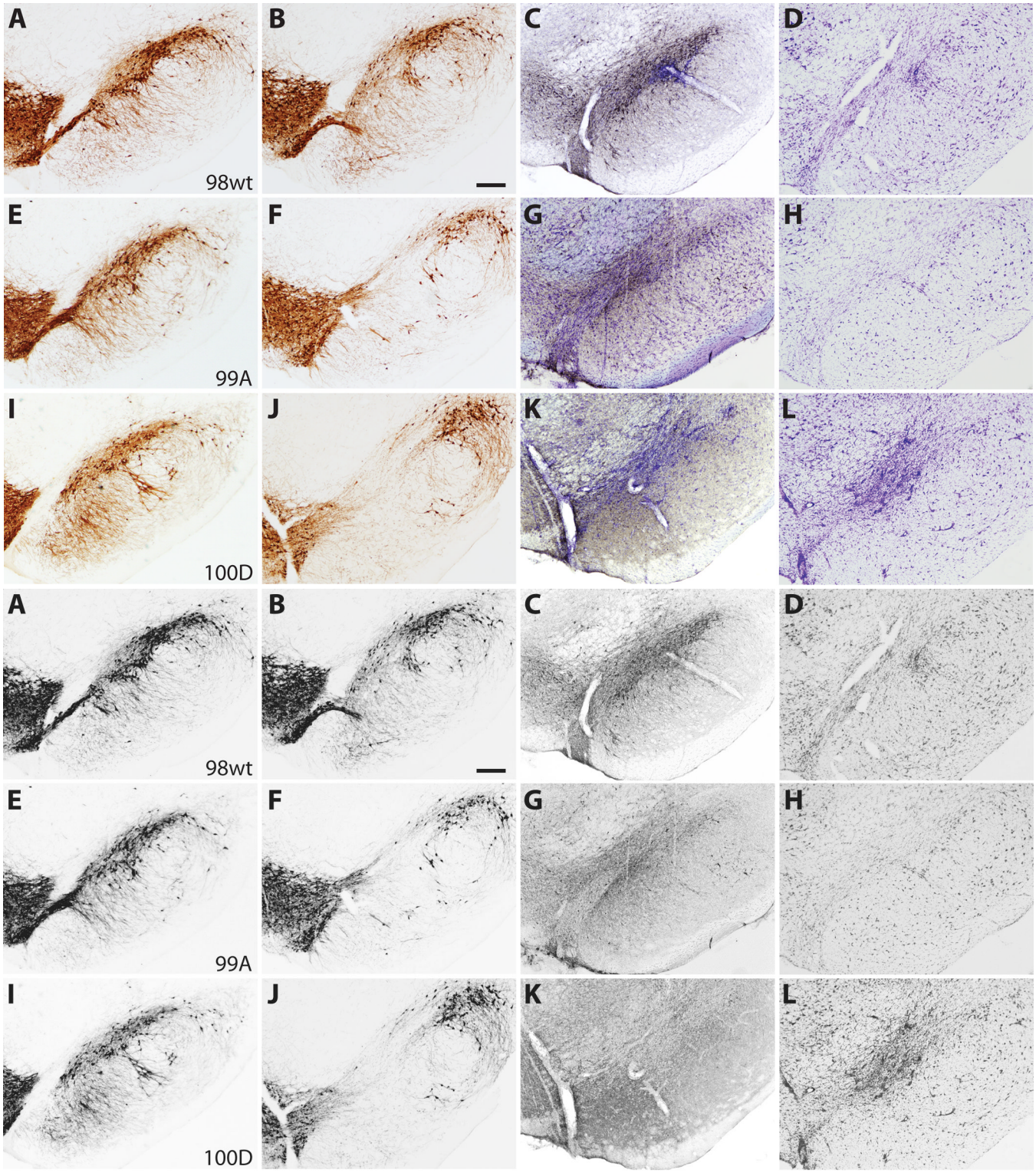

Figure 4.

Photomicrographs of representative substantia nigra (SN) sections at 6 weeks post-injection demonstrate neurodegenerative changes and tyrosine hydroxylase (TH) cell loss. (**A–D)** Case 98, wild type (wt) ⟨-synuclein. (**E–H)** Case 99, S129A. (**I–L)** Case 100, S129D. (**A, E, I)** TH

immunostaining in the contralateral SN after empty vector control injection. (**B, F, J)** TH cell loss in the SN for wt and S129 mutant cases. (**C, G, K**) Distribution of human ⟨-synuclein (LB509) expression (gray-black immunostaining) within the SN. (**D, H, L**) Adjacent sections stained with cresyl violet that demonstrate SN cell loss and gliosis at rAAV injection sites. Bar: 250 ⌠m.

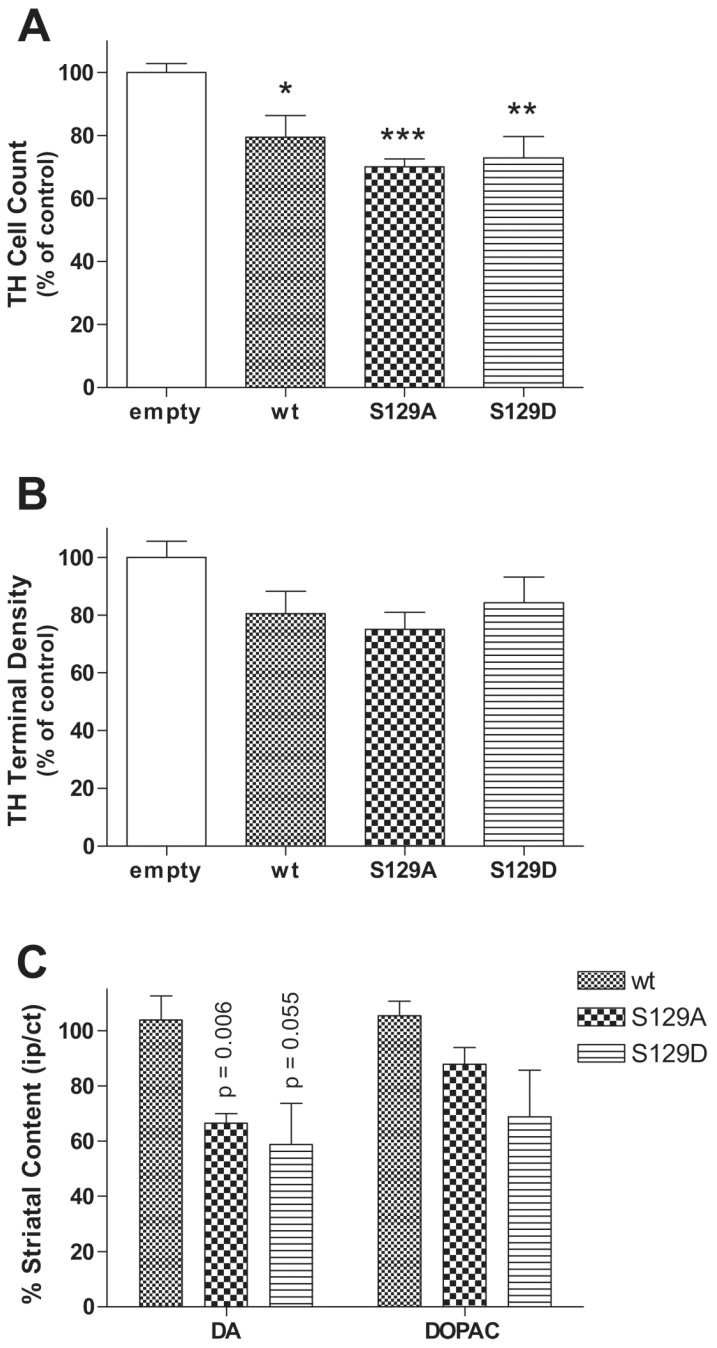

Figure 5.

Graphs of nigral tyrosine hydroxylase (TH) cell loss, striatal TH terminal density, and dopamine content. (**A**) Stereological estimates of TH cell loss in the SN at 6 weeks are expressed relative to empty vector control. Expression of both wild type (wt) and S129 mutant ⟨-synuclein resulted in significant TH cell loss (mean 25.8%) compared to control (*$p < 0.05$, **$p < 0.01$, ***$p < 0.001$; $F[3,24] = 9.96$, $p = 0.0002$). However, TH cells did not differ among wt and S129A and S129D groups. (**B**) Optical density scan array analysis of striatal TH terminal density showed a 16% to 25% decrease for wt and S129 mutants, but no significant difference among groups ($F[3,27] = 2.514$, $p = 0.080$). (**C**) Relative striatal dopamine (DA) (compared

to contralateral striatum injected with empty vector control) but not 3,4-dihydroxyphenlyacetic acid (DOPAC) content was reduced only in S129 mutants.

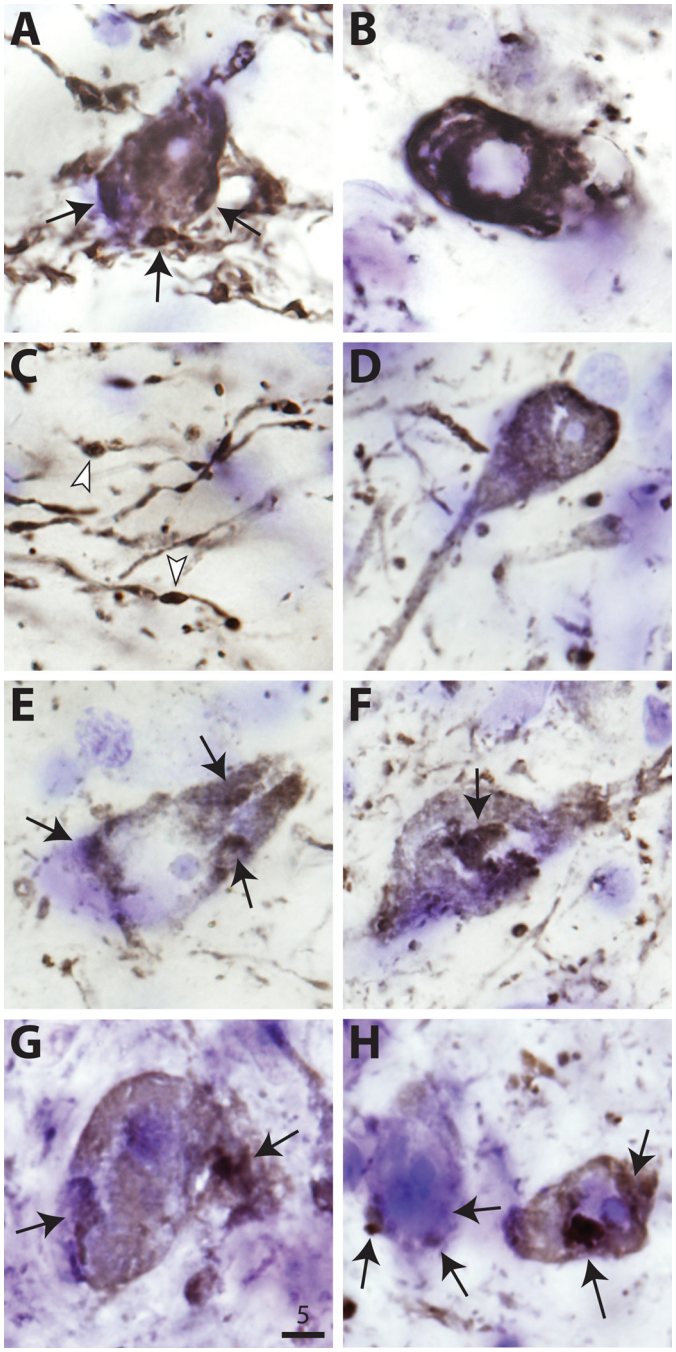

Figure 6.

High-power photomicrographs of human α-synuclein (LB509) immunostaining of nigral neurons in wild type (wt) (**A–C**), S129A (**D–F**), and S129D (**G, H**) recipients. Arrows indicate large intracytoplasmic ⟨-synuclein-positive aggregates. Most aggregates were either perinuclear or in the periphery (**A** and **G**). **B** shows typical nuclear ghosting, consistent with neurodegenerative change. Dystrophic neurites in **C** have characteristic α-synuclein-positive inclusions (arrowheads). Bar: 5 ⌠m.